A. Conservative analysis of Bni1 among fungi species

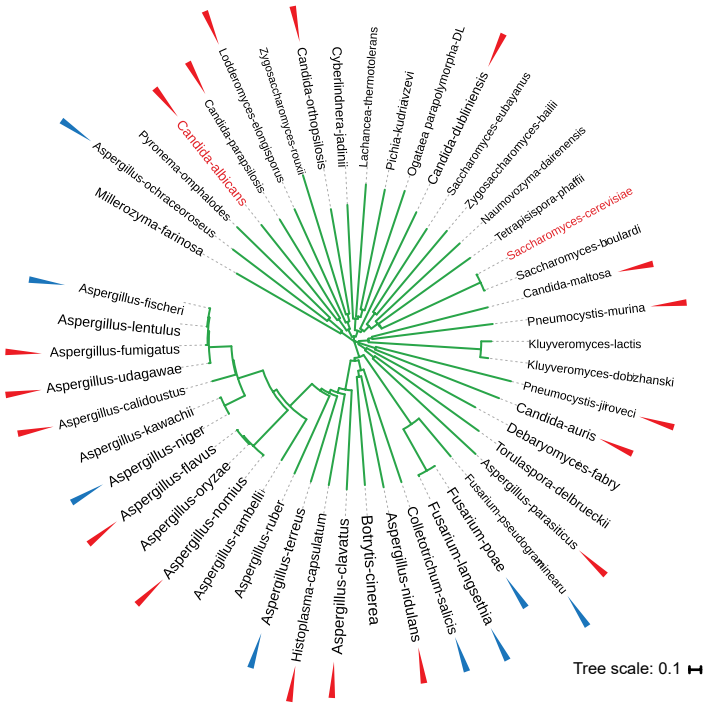

B. Conservative analysis of Bud6 among fungi species

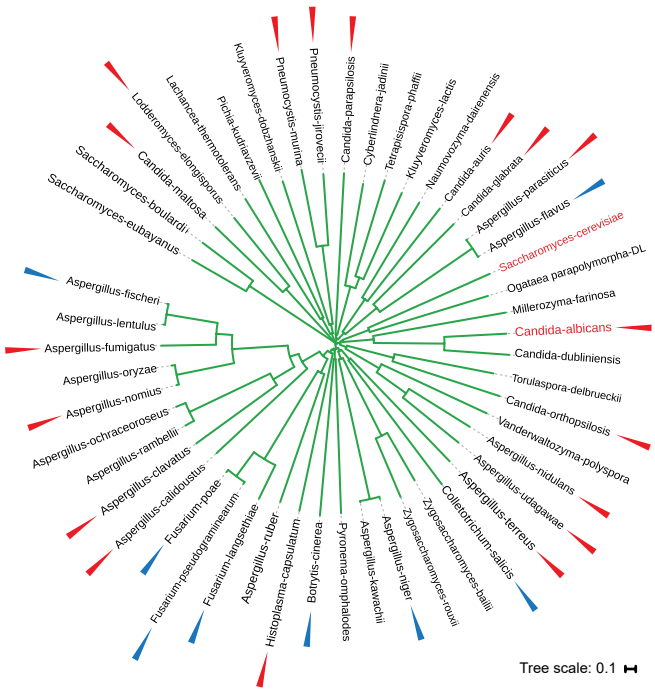

C. Conservative analysis of Spa2 among fungi species

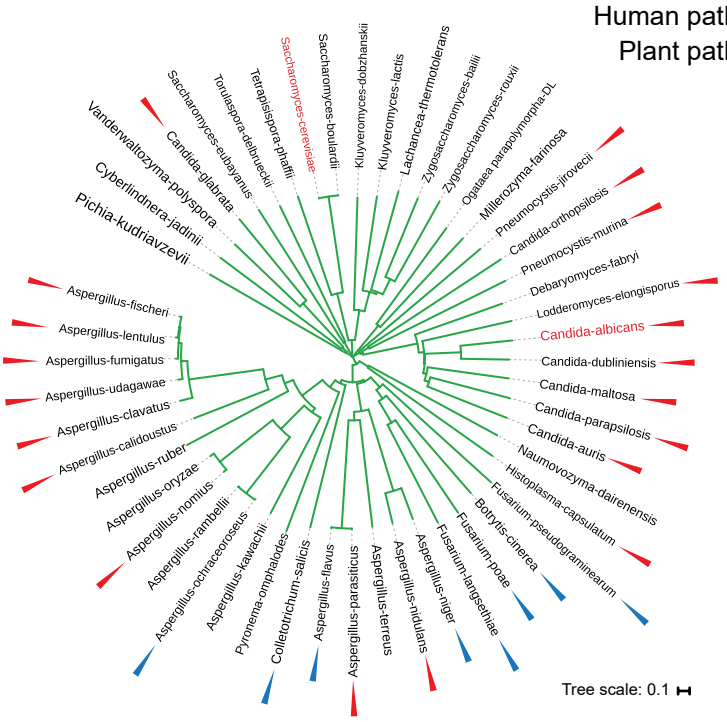

D

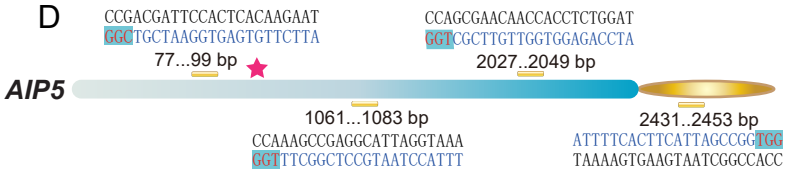

E

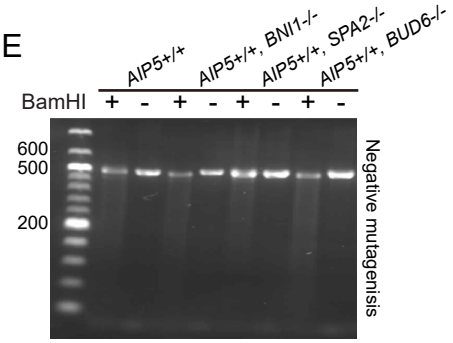

F

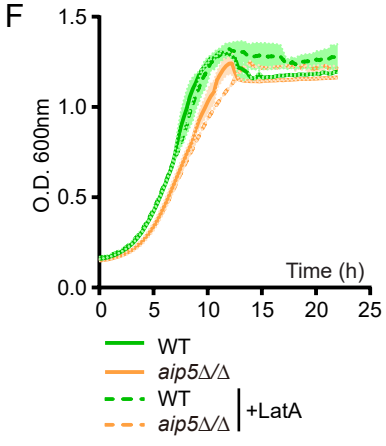

G

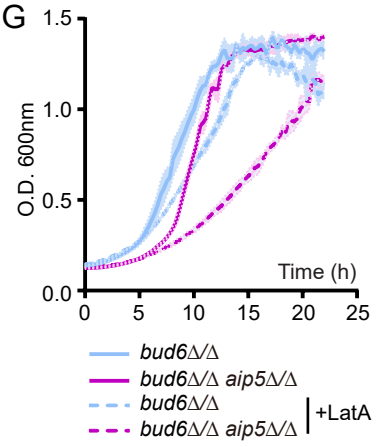

H

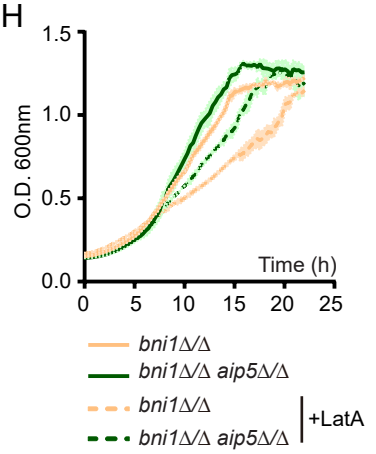

I

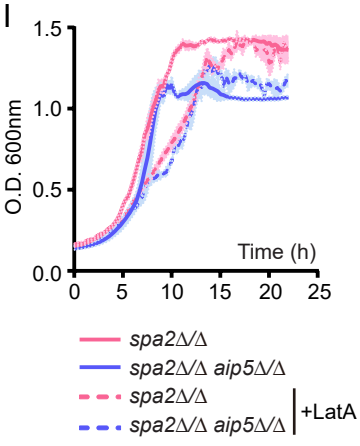

Supplementary figure 1. Polarisome proteins are conserved among fungi species.

(A-C) Phylogenetic tree of polarisome proteins Bni1, Bud6 and Spa2, the two highlighted species in red are *S. cerevisiae* and *C. albicans*. (D) Four gRNA sequences with *AIP5*-specific target sequences as indicated. A stop codon and a BamHI cleavage site were inserted at the location immediately following the correct mutagenesis site (highlighted by a red star) located at the 76 bp region. (E) The negative control of CRISPR/Cas9 edited *AIP5* in various *C. albicans* wild type and mutant strains, where no BamHI digestion sites were inserted at the target location. (F-I) Growth curve of the indicated polarisome *C. albicans* mutants that were treated with or without 1 μM latrunculin A. The data were averaged with four technical replicates and showed with an error bar of S.D.

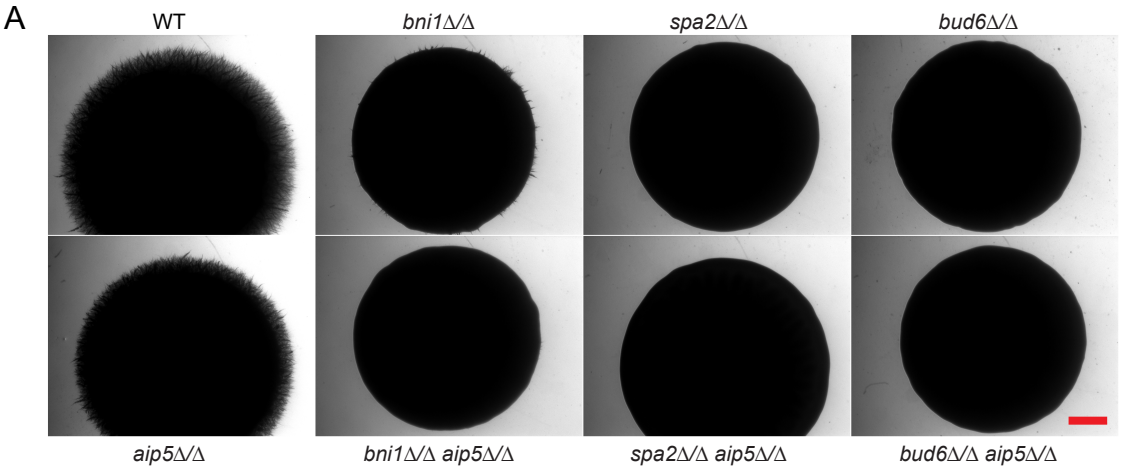
A
WT
bni1Δ/Δ
spa2Δ/Δ
bud6Δ/Δ
aip5Δ/Δ
bni1Δ/Δ aip5Δ/Δ
spa2Δ/Δ aip5Δ/Δ
bud6Δ/Δ aip5Δ/Δ

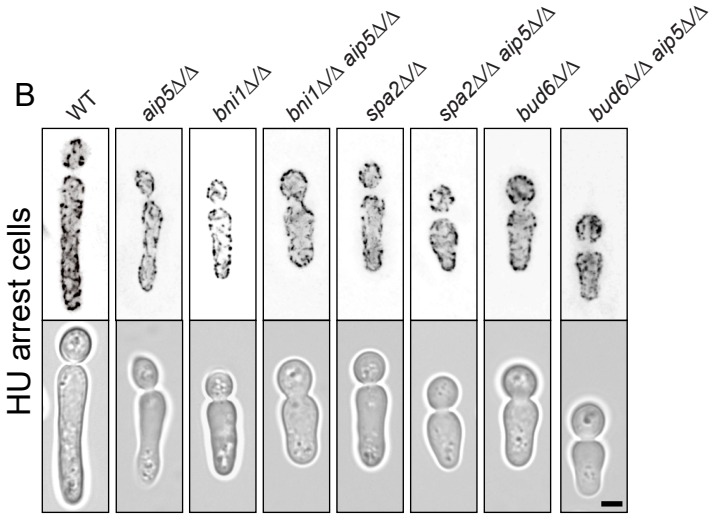
B
HU arrest cells
WT
aip5Δ/Δ
bni1Δ/Δ
bni1Δ/Δ aip5Δ/Δ
spa2Δ/Δ
spa2Δ/Δ aip5Δ/Δ
bud6Δ/Δ
bud6Δ/Δ aip5Δ/Δ

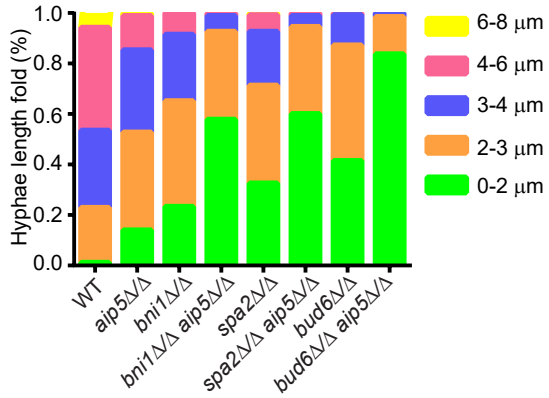
C
Hyphae length fold (%)
1.0
0.8
0.6
0.4
0.2
0.0
6-8 μm
4-6 μm
3-4 μm
2-3 μm
0-2 μm
WT
aip5Δ/Δ
bni1Δ/Δ
bni1Δ/Δ aip5Δ/Δ
spa2Δ/Δ
spa2Δ/Δ aip5Δ/Δ
bud6Δ/Δ
bud6Δ/Δ aip5Δ/Δ

Supplementary figure 2. Polarisome mutants reduced hyphae growth length.

(A) Representative images of the indicated strain colonies with hyphae cells induced by solid agar spider plate at 37°C. The images were shown with a magnification of 12 x, the scale bar represents 2 cm. (B) The representative fluorescence images of actin pattern stained by phalloidin 488 in the indicated mutants of hydroxyurea (HU)-induced polarized filaments (upper panel), and bright-field images of cell morphology (lower panel). Images were acquired from paraformaldehyde-fixed cells after 5 hours of HU induction. The scale bar represents 2 μm. (C) Quantification of HU-induced polarized filament length by measuring the distance between bud-neck and bud-tip. The filament length was classified into five groups. The distribution in the percentage of each group was shown in the indicated strains. n=250 cells for each strain.

Supplementary figure 3

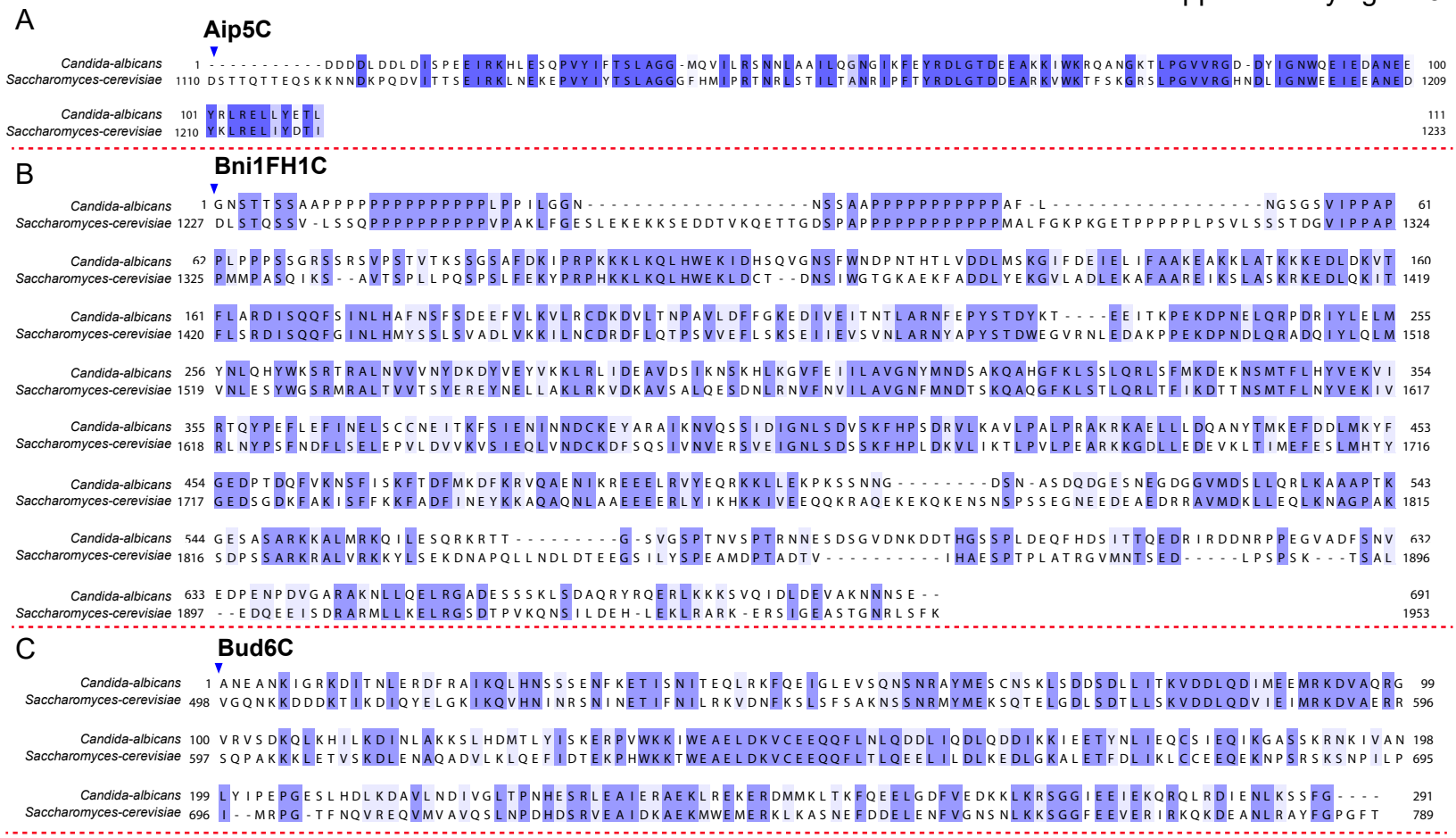

Supplementary figure 3. Conservative analysis of polarisome proteins among fungi species.

(A-C) The functional C terminal domain protein sequence alignment of Aip5, Bni1, and Bud6 between *S. cerevisiae* and *C. albicans*.

Supplementary figure 4

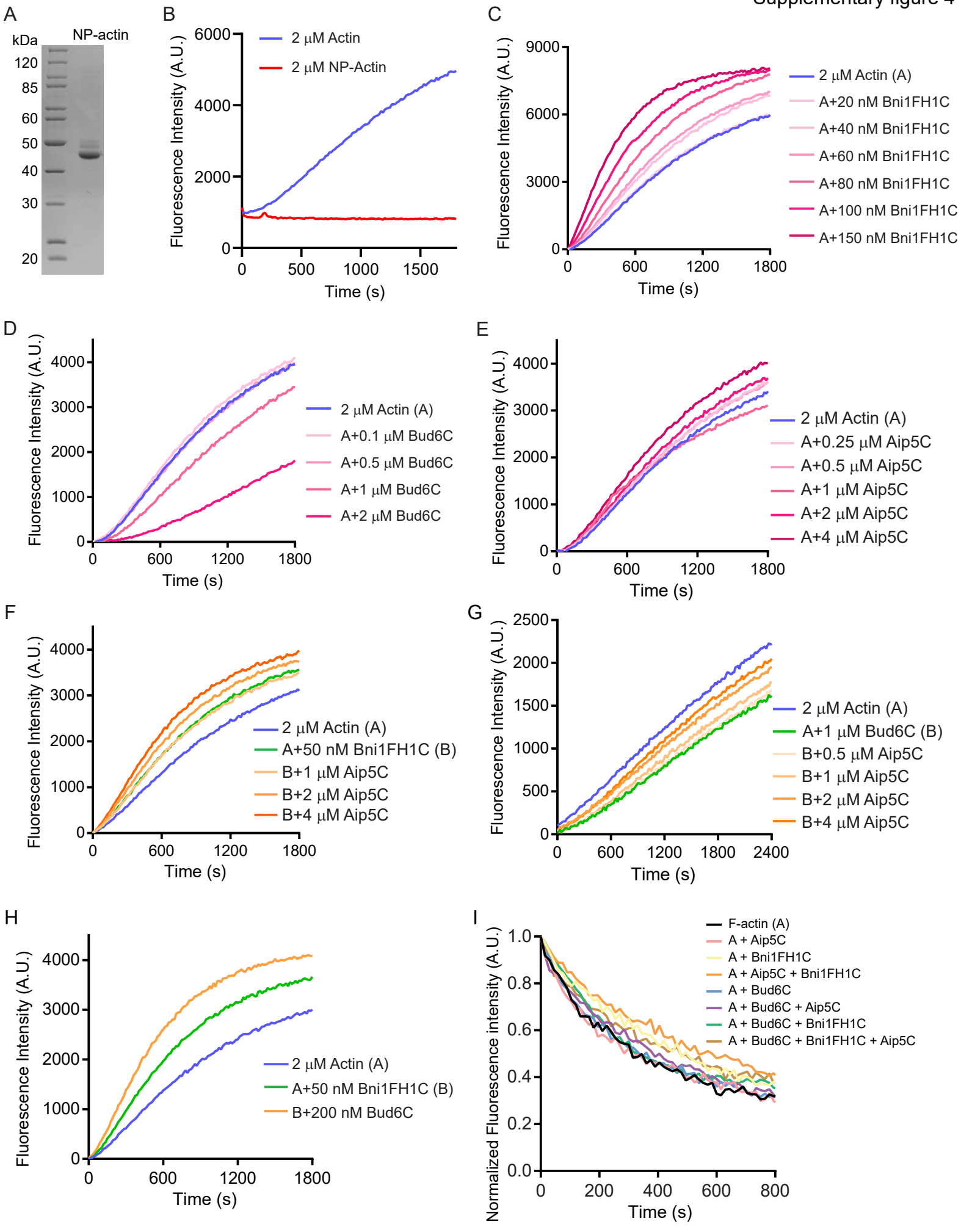

Supplementary figure 4. Polarisome proteins work synergistically to enhance actin assembly *in vitro.*

(A) SDS-PAGE gel of purified NP-actin (*S. cerevisea* actin with D286A, V287A, D288A mutations). (B) Pyrene actin polymerization test of NP-actin. (C-E) Pyrene actin polymerization assays of an increasing concentration of Bni1FH1C, Bud6C, and Aip5C, respectively. (F, G) Pyrene actin polymerization by an increasing concentration of Aip5C in combination with Bni1FH1C (F) or Bud6C (G). (H) Pyrene actin polymerization by an increasing concentration of Bud6C in combination with Bni1FH1C. (I) Pyrene actin depolymerization assay of the indicated proteins.

Supplementary figure 5

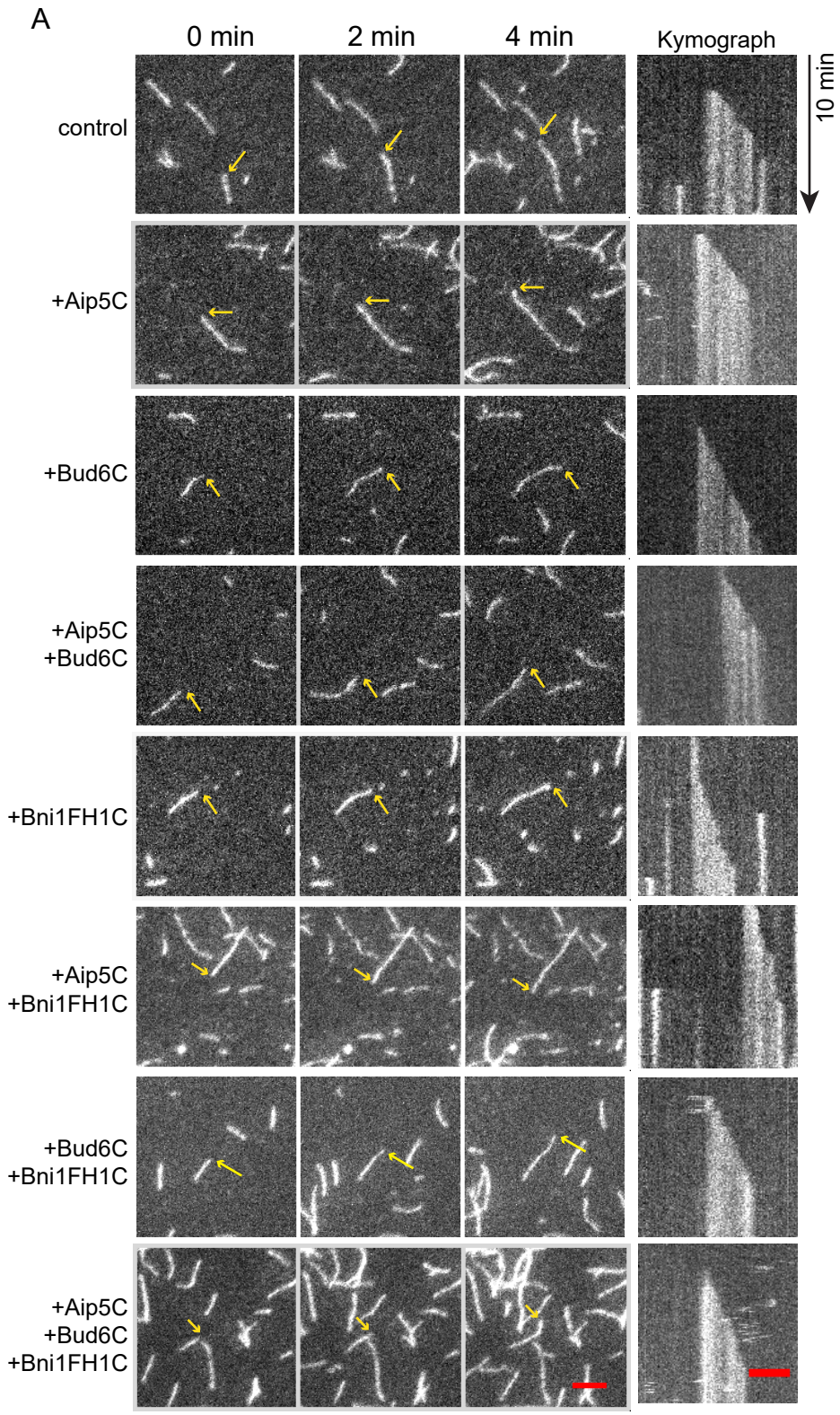

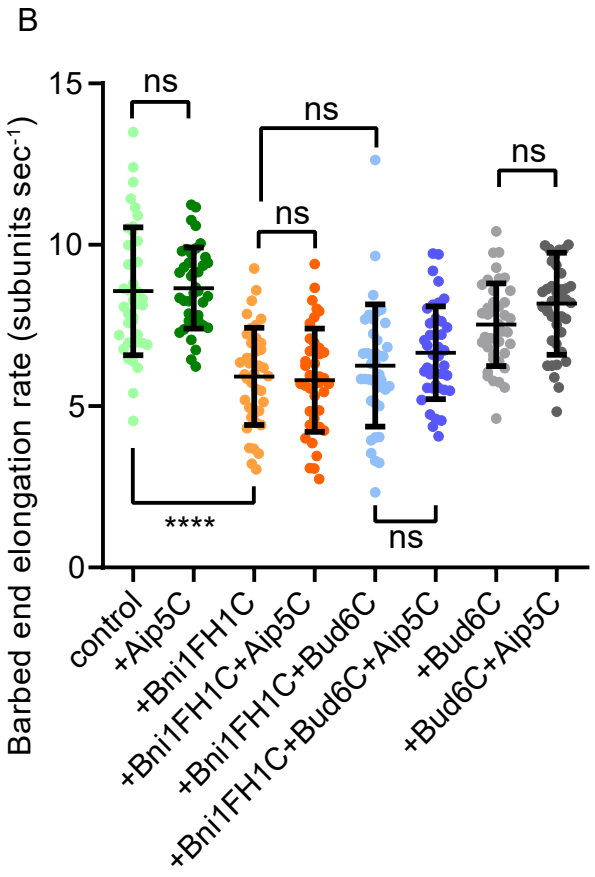

Supplementary figure 5. The effect of polarisome proteins on actin filament barbed end elongation speed.

(A) The representative TIRF images of elongating actin filaments at the indicated time points. The kymographs were generated from movies covering 10 min with 5-sec gaps in between each frame. The control actin filament was assembled from 0.5 μM actin (10% Oregon green 488 labelled actin and 0.5% biotin-actin), and the proteins added were indicated as follows: 20 nM Bni1FH1C; 10 nM Aip5C and 10 nM Bud6C. The scale bar represents 5 μm. (B) Quantification of actin filament barbed end elongation speed of indicated protein combinations as shown in A. (n=40 for each sample) P-values was determined by the one-way ANOVA, ns=not significant, ****$p < 0.0001$. Error bar, S.D.

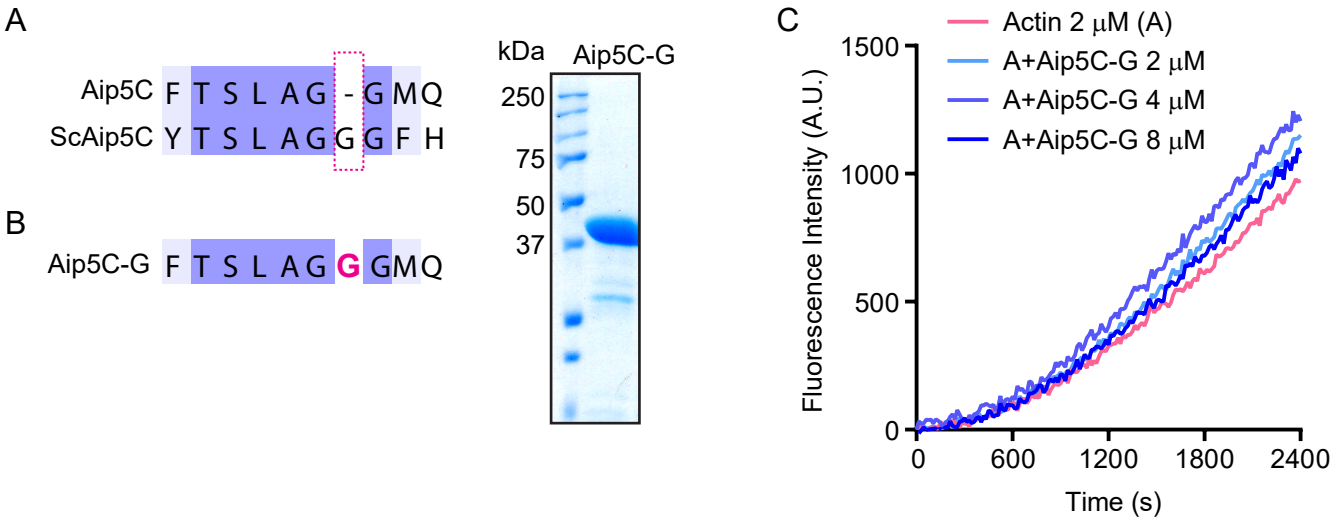
A
Aip5C F T S L A G - G M Q
ScAip5C Y T S L A G G G F H
B
Aip5C-G F T S L A G G G M Q
kDa
Aip5C-G
250
75
50
37
C
Actin 2 μM (A)
A+Aip5C-G 2 μM
A+Aip5C-G 4 μM
A+Aip5C-G 8 μM
Fluorescence Intensity (A.U.)
1500
1000
500
0
0
600
1200
1800
2400
Time (s)

Supplementary figure 6. Aip5C mutants and activation in actin assembly.

(A) Protein sequence comparison of the functional loop domain between *C. albicans* and *S. cerevisiae*. (B) The protein sequence of Aip5C-G where the Glycine was inserted. The purified Aip5C-G was shown in SDS-PAGE. (C) The bulk actin assembly was tested by pyrene assay with increasing concentrations of Aip5C-G.

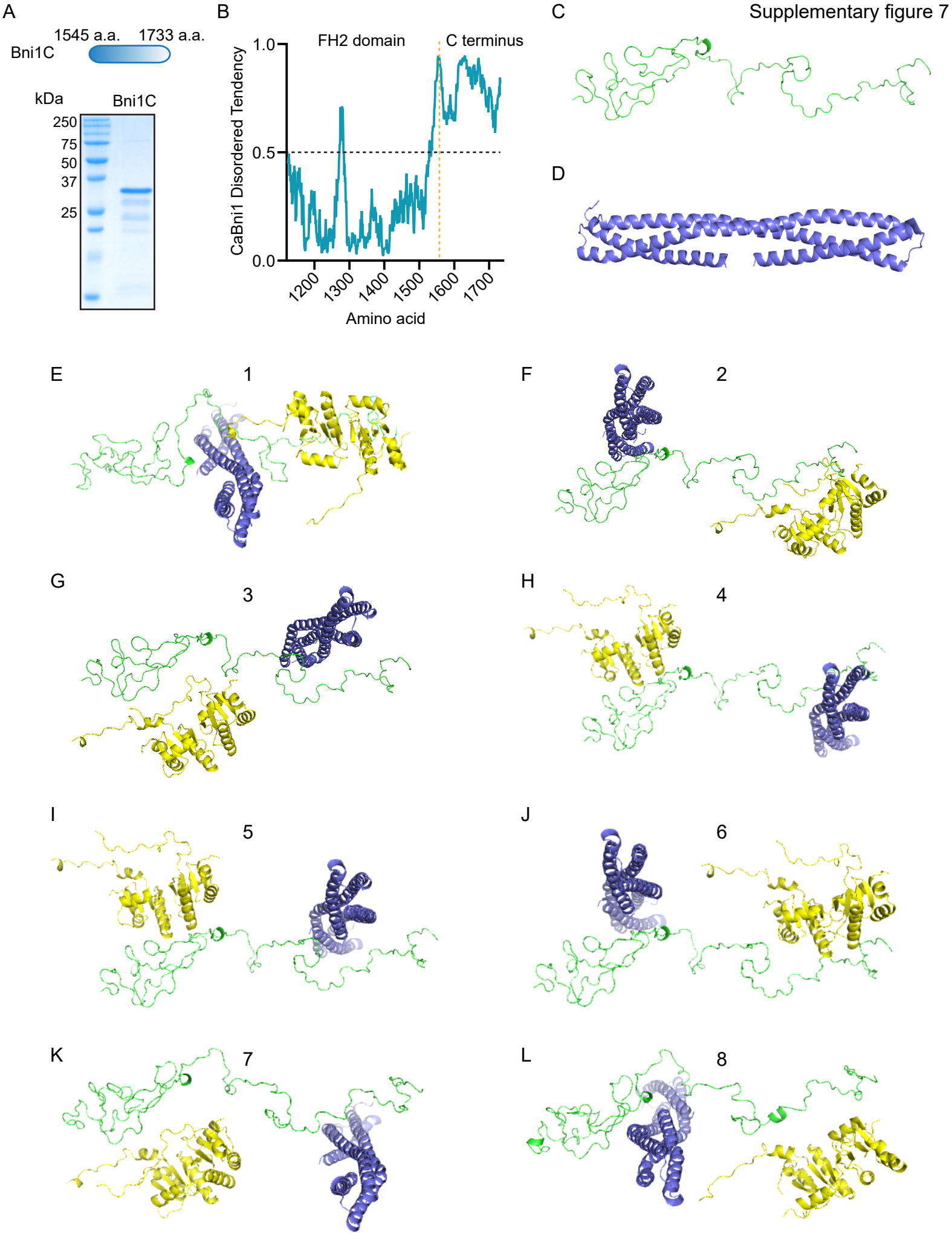
A
1545 a.a.
1733 a.a.
Bni1C
kDa
Bni1C
250
75
50
37
25
B
FH2 domain
C terminus
CaBni1 Disordered Tendency
1.0
0.5
0.0
1200
1300
1400
1500
1600
1700
Amino acid
C
D
E
1
F
2
G
3
H
4
I
5
J
6
K
7
L
8

Supplementary figure 7. Initial Bni1C-Bud6C-Aip5C complex structure placements for MD simulations

(A) The recombinant Bni1C (residues 1545-1733 a.a.) was purified and shown in SDS-PAGE. (B) The intrinsically disordered tendency plot of protein Bni1FH1COOH by using IUPRED2A. While Bni1C is highly disordered, the FH2 domain is predicted to be well folded as the disorder tendency score is lower than 50%. (C, D) The initial structure in MD simulations for Bni1C (C) and Bud6C (D). (E-L) The initial eight sets of Bni1C-Bud6C-Aip5C complex placements, where Bni1C was placed along the x-axis with N terminus on the left side, and Aip5C and Bud6C were assigned into four directions (right, left, up, and down) relative to Bni1C.

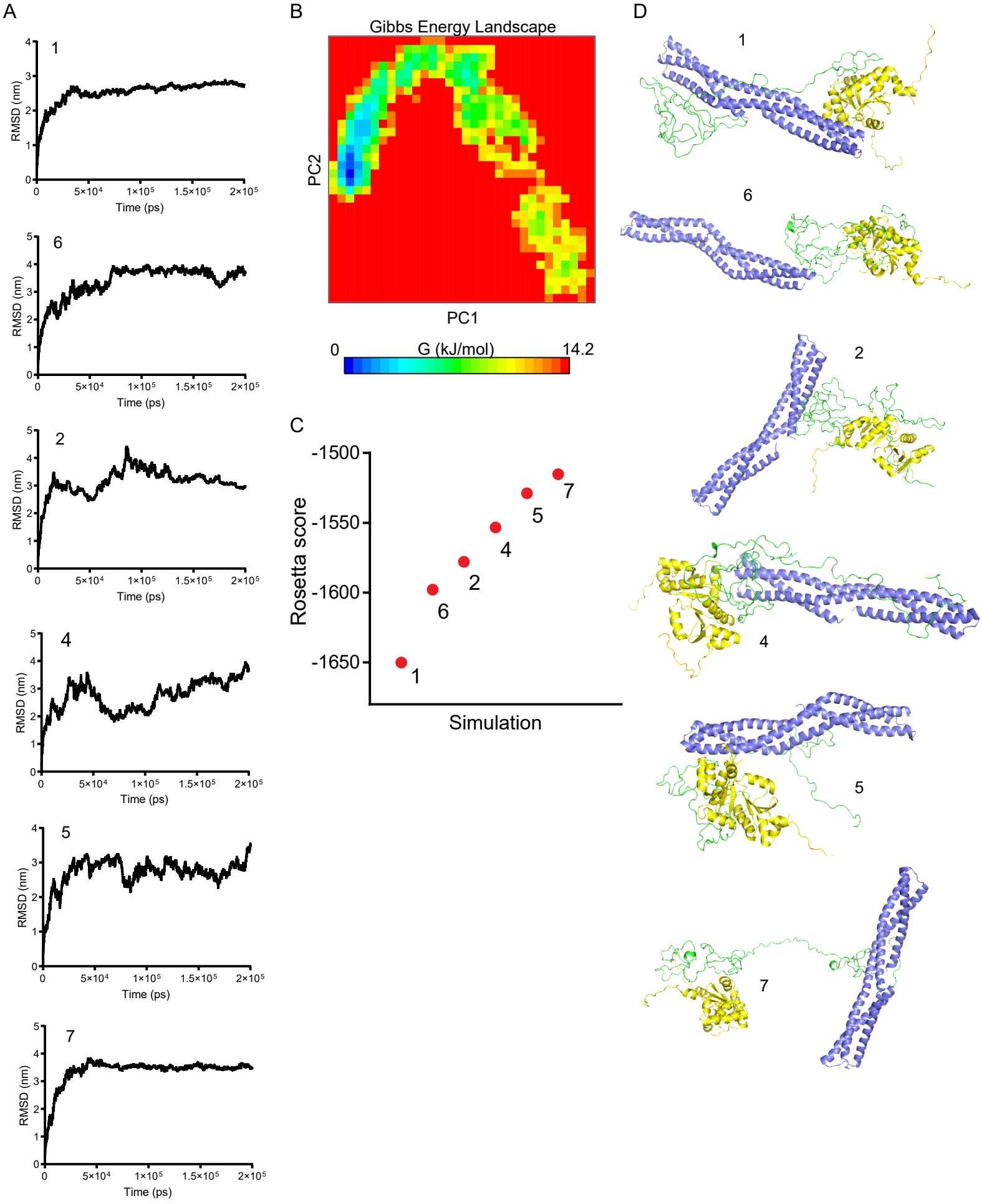
A
1
RMSD (nm)
Time (ps)
6
2
4
5
7
B
Gibbs Energy Landscape
PC2
PC1
0
G (kJ/mol)
14.2
C
Rosetta score
-1500
-1550
-1600
-1650
Simulation
D

Supplementary figure 8. The RMSD plots and Rosetta scoring of the stable tri-protein complex from MD simulations

(A) The RMSD plots of six groups (Simulation 1, 2, 4, 5, 6, 7) that maintain stable complex conformations after MD simulations. Simulation 3 and 8 complexes were excluded because of the full or partial detachments of three proteins after MD simulations. (B) Free energy landscape of the first two Principle components（PC1 and PC2) for the tri-complexes (Simulation 1). The energy scale representing the stable (Blue) to least stable (Red) structures ranging from 0 to 14.2 kcal/mol. (C) The Rosetta scores of the six sets of tri-protein complex after MD simulations. (D) The conformations of the most stable assembly of tri-protein complex for each set (including conformation 1 in figure 6C).

Supplementary Table 1. Yeast strains used in this study.

Strain name	Genotype	Source
YMY2045 (BWP17)	*ura3/ura3 his1::hisG/his1::hisG arg4::hisG/arg4::hisG*	(1)
YMY2046	BWP17 *spa2*Δ::*ARG4*/*spa2*Δ::*FRT*	(2)
YMY2047	BWP17 *bni1Δ::ARG4/bni1Δ::HIS1*	(3)
YMY2048	BWP17 *bud6Δ::ARG4/bud6Δ::HIS1*	(3)
YMY2049	BWP17 *aip5Δ:: NATR/aip5Δ:: NATR*	This study
YMY2050	BWP17 *spa2Δ::ARG4/spa2Δ::FRT aip5Δ:: NATR/aip5Δ:: NATR*	This study
YMY2051	BWP17 *bni1Δ::ARG4/bni1Δ::HIS1 aip5Δ:: NATR/aip5Δ:: NATR*	This study
YMY2052	BWP17 *bud6Δ::ARG4/bud6Δ::HIS1 aip5Δ:: NATR/aip5Δ:: NATR*	This study

Supplementary Table 2. Oligonucleotide primers used in the study.

SgAIP5-F	ATTCTTGTGAGTGGAATCGTGTTTTAGAGCTAGAAATAGCAAGTTAAAA
SgAIP5-R	ACGATTCCACTCACAAGAATCGGATCCAAATTAAAAATAGTTTACGCAA GT
RtAIP5-F	TCCATCTTTGGTTGGATCTTCCATTAGATCATAAGGATCCACGATTCCACT CACAAGAAT
RtAIP5-R	TGATATCTTTGGAAGATTTGTATTTTTCTGGGTGGATATAATTCTTGTGAG TGGAATCGT
VerAIP5-F	GACATTGAAGAGCGTTTAG
VerAIP5-R	TTTACCTCCAACATTATCAG

1. Wilson, R. B., Davis, D., and Mitchell, A. P. (1999) Rapid hypothesis testing with Candida albicans through gene disruption with short homology regions. *Journal of bacteriology* **181**, 1868-1874
2. Wang, H., Huang, Z. X., Au Yong, J. Y., Zou, H., Zeng, G., Gao, J., Wang, Y., Wong, A. H. H., and Wang, Y. (2016) CDK phosphorylates the polarisome scaffold Spa2 to maintain its localization at the site of cell growth. *Molecular microbiology* **101**, 250-264

3. Li, C. R., Wang, Y. M., De Zheng, X., Liang, H. Y., Tang, J. C. W., and Wang, Y. (2005) The formin family protein CaBni1p has a role in cell polarity control during both yeast and hyphal growth in Candida albicans. *Journal of cell science* **118**, 2637-2648